

# Concentration dependence of the Néel temperature of $\text{Mn}_{100-x}\text{Rh}_x$ ordered alloys

R. Yamauchi<sup>a</sup>, K. Fukamichi<sup>a,\*</sup>, H. Yamauchi<sup>b</sup>, A. Sakuma<sup>c</sup>

<sup>a</sup>Department of Materials Science, Graduate School of Engineering, Tohoku University, Aoba-yama 02, Sendai 980-8579, Japan

<sup>b</sup>Institute of Material Research, Tohoku University, Katahira, Sendai 980-8577, Japan

<sup>c</sup>Magnetic and Electric Materials Research Laboratory, Hitachi Metals, Ltd., Mikajiri 5200, Kumagaya, Saitama 360-0843, Japan

Received 6 May 1998

---

## Abstract

Concentration dependences of the room temperature lattice constant and the Néel temperature of  $\text{Mn}_{100-x}\text{Rh}_x$  ( $19 \leq x \leq 30$ ) ordered alloys were investigated. The room temperature lattice constant becomes larger with increasing  $x$ . The Néel temperature also increases with the increase of  $x$ , and the high Néel temperature is not explained by an exchange interaction as a function of the Mn–Mn distance, but by the number of 3d electrons in the Mn site. Associated with spin fluctuations, the paramagnetic susceptibility increases with increasing temperature and shows a tendency to be saturated. © 1998 Elsevier Science S.A. All rights reserved.

**Keywords:** Mn–Rh alloys; Lattice constant; Néel temperature; Magnetic susceptibility; Ordered alloy

---

## 1. Introduction

Recently, Mn and Cr antiferromagnetic alloys have been investigated intensively from the viewpoint for an application to a spin-valve layer of GMR heads [1–6], because they have a high Néel temperature about a few hundreds Kelvin. Some Mn-based alloys have been known to exhibit the lattice distortion associated with a martensitic transformation [7–9]. Furthermore, their structural and magnetic transition temperatures are very sensitive to both heat and mechanical treatments [10]. For practical applications, it is very important to make systematic investigations of fundamental magnetic properties for Mn-based antiferromagnets.

In the present study, we focus our interest on a  $\text{AuCu}_3$ -type  $\text{Mn}_3\text{Rh}$  ordered alloy system, because the Néel temperature of a stoichiometric  $\text{Mn}_3\text{Rh}$  ordered alloy [11] is higher than that of other Mn alloy systems such as  $\text{Mn}_3\text{Pt}$  [12,13],  $\text{Mn}_3\text{Fe}$  [14,15],  $\text{Mn}_3\text{Ni}$  [16] and  $\text{Mn}_3\text{Pd}$  [17]. According to the phase diagram of Mn–Rh system, the  $\text{AuCu}_3$ -type  $\text{Mn}_3\text{Rh}$  ordered-phase exists in the concentration range from 11 to 32% Rh [18]. The stoichiometric  $\text{Mn}_3\text{Rh}$  ordered alloy is obtained below about 1130

K, and its Néel temperature and the magnetic structure were investigated by neutron scattering [11]. The data revealed that  $\text{Mn}_3\text{Rh}$  ordered alloy has a non-collinear triangular antiferromagnetic structure and the second nearest neighbor Mn atoms align ferromagnetic. However, the reason why the  $\text{Mn}_3\text{Rh}$  ordered alloy shows such a high Néel temperature has not been clear yet. It is interesting to investigate the magnetic properties by changing the distance of the Mn atoms and/or the number of 3d electrons in the Mn site. Therefore, we have carried out the room temperature X-ray diffraction analyses and magnetic measurements from room temperature to about 1100 K for  $\text{Mn}_{100-x}\text{Rh}_x$  ( $19 \leq x \leq 30$ ) ordered alloys.

## 2. Experimental

The specimens were prepared by arc-melting in an argon gas atmosphere purified with a Ti getter. The ingots were turned over and remelted four times. In order to homogenize they were annealed for 240 h at 873 K in an evacuated-quartz tube and subsequently quenched into ice-water. The room temperature lattice constant was examined by X-ray powder diffraction method. The magnetic measurements

---

\*Corresponding author.

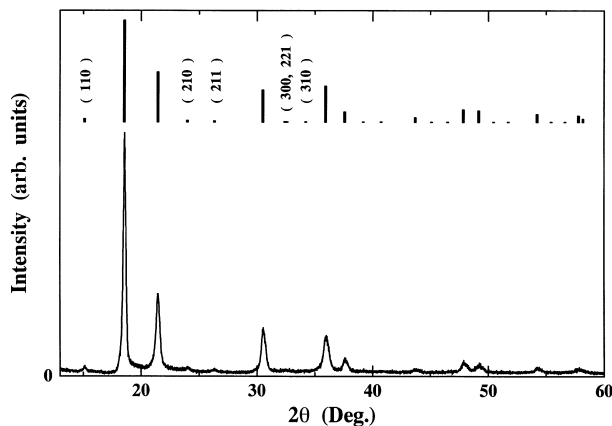


Fig. 1. Powder X-ray diffraction pattern of  $\text{Mn}_{75}\text{Rh}_{25}$  ordered alloy, together with the calculated intensities.

were carried out with a VSM from room temperature to about 1100 K.

### 3. Results and discussion

X-ray powder diffraction pattern of  $\text{Mn}_{75}\text{Rh}_{25}$  ( $\equiv \text{Mn}_3\text{Rh}$ ) ordered alloy and calculated reflection intensities are shown in Fig. 1. The indices of the superlattice lines below about  $2\theta=30$  are given in the same figure. Their integrated reflection intensities nearly correspond to the calculated ones. Further, the ordered state was confirmed by electron diffraction [19]. In Fig. 2 the room temperature lattice constant of  $\text{Mn}_{100-x}\text{Rh}_x$  ( $19 \leq x \leq 30$ ) ordered alloys as a function of  $x$  is shown. The lattice constant increases with increasing  $x$ , and the value of the stoichiometric  $\text{Mn}_3\text{Rh}$  ordered alloy is 3.815 Å, in good agreement with the reported result [11].

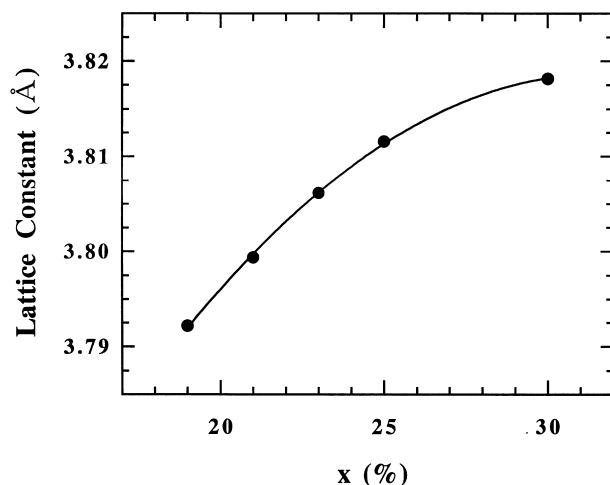


Fig. 2. The room temperature lattice constant of  $\text{Mn}_{100-x}\text{Rh}_x$  ( $19 \leq x \leq 30$ ) ordered alloys as a function of  $x$ .

In Fig. 3 the temperature dependence of magnetic susceptibility from 650 to 1000 K for the  $\text{Mn}_{100-x}\text{Rh}_x$  ( $x=19, 21, 23$  and  $25$ ) ordered alloys is shown. In the figure, a clear peak due to the magnetic transition is observed at 802, 819, 827 and 841 K for  $x=19, 21, 23$  and  $25$  alloys, respectively. The paramagnetic susceptibility of these alloys increases and indicates a tendency to be saturated, showing that the magnetic susceptibility does

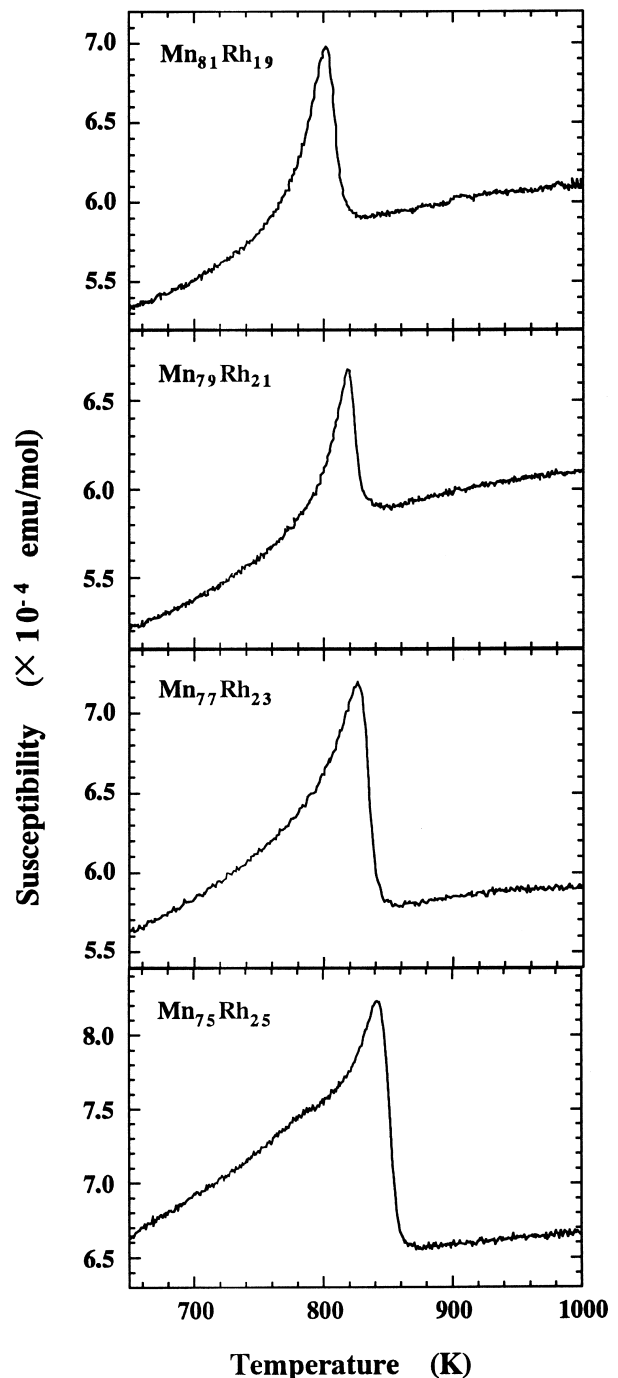


Fig. 3. Temperature dependence of the magnetic susceptibility of  $\text{Mn}_{100-x}\text{Rh}_x$  ( $x=19, 21, 23$  and  $25$ ) ordered alloys.

not follow the Curie–Weiss law. The increase of the paramagnetic susceptibility has been observed in  $\text{YMn}_2$  [20] and  $\text{Mn}_3\text{Pt}$  [21]. For  $\text{YMn}_2$  compound, this behavior has been explained as a weak itinerant-electron magnetic property, that is, the mean-square local amplitude of spin fluctuation  $S_L^2$  is increased by thermal fluctuations in the paramagnetic region [22]. The itinerant-electron characters of  $\text{Mn}_3\text{Pt}$  ordered alloy have been discussed by using a band structure [23] and also a spin-wave dispersion [24]. The increase of the paramagnetic susceptibility of  $\text{Mn}_{100-x}\text{Rh}_x$  ordered alloys would also be explained by the spin fluctuations characterized in itinerant-electron systems.

Shown in Fig. 4 is the relation between the Néel temperature and the room temperature lattice constant of the stoichiometric  $\text{Mn}_3\text{Rh}$ , together with that of  $\text{Mn}_3\text{Pt}$  and  $\text{Mn}_3(\text{Pt}_{0.5}\text{Rh}_{0.5})$  [11] and  $\text{Mn}_3\text{Ir}$  [25] ordered alloys. It is clear that the smaller the lattice constant, the higher the Néel temperature. The magnitude of the Néel temperature, namely, the strength of the exchange interaction, appears to be related with the Mn–Mn distance. Yamada et al. have calculated the exchange interaction  $J(r)$  as a function of the Mn–Mn distance [26]. According to their calculation,  $J(r)$  takes a minimum around 2.5 Å and changes the sign from negative to positive around 3.0 Å. This means that the exchange interaction becomes weaker with increasing the lattice constant for Mn-based alloys.

In Fig. 5 the concentration dependence of the Néel temperature of  $\text{Mn}_{100-x}\text{Rh}_x$  ( $19 \leq x \leq 30$ ) ordered alloys is shown. The Néel temperature becomes higher with increasing  $x$ . The present value of the stoichiometric  $\text{Mn}_3\text{Rh}$  ordered alloy is practically consistent with the value reported before [11], although the heat-treatment is slightly different. The concentration dependence of the Néel temperature for  $\text{Mn}_{100-x}\text{Pt}_x$  [12,13],  $\text{Mn}_{100-x}\text{Fe}_x$  [14,15],  $\text{Mn}_{100-x}\text{Ni}_x$  [16] and  $\text{Mn}_{100-x}\text{Pd}_x$  [17] seems to be ex-

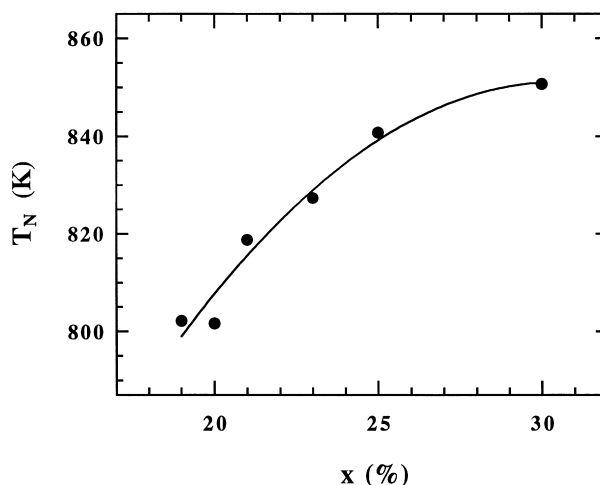


Fig. 5. Concentration dependence of the Néel temperature of  $\text{Mn}_{100-x}\text{Rh}_x$  ( $19 \leq x \leq 30$ ) ordered alloys.

plained within the framework of  $J(r)$ , that is to say, the larger the lattice constant, the lower the Néel temperature. From Figs. 2 and 5, however, the larger the lattice constant, the higher the Néel temperature for the present  $\text{Mn}_{100-x}\text{Rh}_x$  ordered alloys. Similar behavior has been reported for  $\text{Mn}_{100-x}\text{Ir}_x$  disordered alloys [25]. Their magnetic structure and the Mn concentration dependence of the Néel temperature were investigated by neutron scattering and magnetic measurements [27]. The stoichiometric  $\text{Mn}_3\text{Ir}$  disordered alloy has a collinear antiferromagnetic structure and (001) ferromagnetic layers stacked antiferromagnetically. On the other hand, the  $\text{Mn}_3\text{Rh}$  ordered alloy has a non-collinear triangular antiferromagnetic structure, mentioned before [11]. Therefore, it is considered that the difference of the magnetic structure between  $\text{Mn}_3\text{Rh}$  and  $\text{Mn}_3\text{Ir}$  has no relation with the increase of the Néel temperature.

It has been presumed that a strong perturbation to the band structure is responsible for the increase in the Néel temperature of  $\text{Mn}_{100-x}\text{Ir}_x$  disordered alloys, because the explanation on the basis of the Mn–Mn distance is invalid [28]. Two points should be noted. One is that the additional elements of Rh and Ir, which show a similar concentration dependence of the Néel temperature, have the same number of the valence electrons. Another is that the Néel temperature of  $\text{Mn}_{100-x}\text{X}_x$  ( $\text{X} = \text{Ir}, \text{Rh}, \text{Pt}, \text{Fe}, \text{Ni}$  and  $\text{Pd}$ ) alloys tends to converge to that of  $\gamma\text{-Mn}$  [12–17,28]. According to our preliminary examination by band calculations using the LMTO-ASA method, the number of 3d electrons in the Mn site decreases in the sequence  $\text{Mn}_3\text{Pt}$ ,  $\gamma\text{-Mn}$  and  $\text{Mn}_3\text{Rh}$ . Furthermore, the calculation of the magnetic excitation energy based on the multiple scattering theory predicts that the antiferromagnetic exchange interaction of  $\gamma\text{-Mn}$  becomes stronger with decreasing 3d electron number. Consequently, the difference of the Néel temperature between  $\text{Mn}_{100-x}\text{Pt}_x$  and  $\text{Mn}_{100-x}\text{Rh}_x$  is ex-

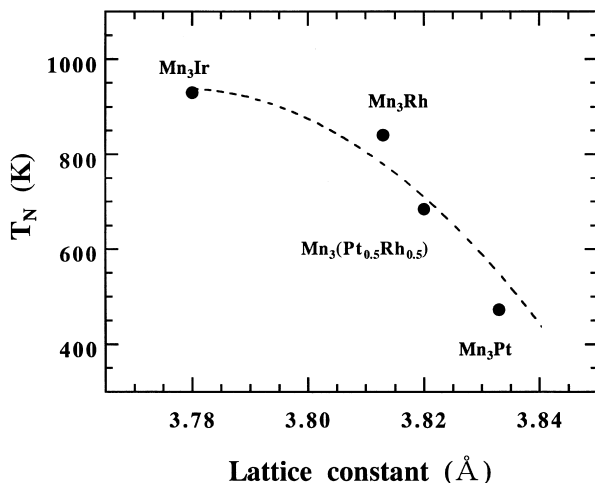


Fig. 4. Relation between the Néel temperature and the room temperature lattice constant with that of  $\text{Mn}_3\text{Pt}$  and  $\text{Mn}_3(\text{Pt}_{0.5}\text{Rh}_{0.5})$  [11] and  $\text{Mn}_3\text{Ir}$  [25] ordered alloys. The dashed line is a guide to the eye.

plained by taking the number of 3d electrons in the Mn site into consideration.

#### 4. Conclusion

We have carried out X-ray powder diffractions analyses at room temperature and the magnetic susceptibility measurements from room temperature to about 1100 K for  $\text{Mn}_{100-x}\text{Rh}_x$  ( $19 \leq x \leq 30$ ) ordered alloys to investigate the concentration dependence of the Néel temperature. The main results are summarized as follows.

1. The room temperature lattice constant of  $\text{Mn}_{100-x}\text{Rh}_x$  ordered alloys becomes larger with increasing  $x$ , showing an increase of the Mn–Mn distance.
2. The paramagnetic susceptibility increases with increasing temperature, and indicates a tendency to be saturated. This behavior could be related with spin fluctuations.
3. The Néel temperature of  $\text{Mn}_{100-x}\text{Rh}_x$  ordered alloys increases with increasing  $x$  in contrast to that of many Mn-based alloys. Such a high Néel temperature is explained by taking the number of 3d electrons in the Mn site into consideration.

#### References

- [1] B. Dieny, V.S. Speriosu, S.S.P. Parkin, B.A. Gurney, D.R. Wilhoit, D. Mauri, *Phys. Rev. B* 43 (1991) 1297.
- [2] T. Lin, D. Mauri, N. Staud, C. Hwang, J.K. Howard, G.L. Gorman, *Appl. Phys. Lett.* 65 (1994) 1183.
- [3] H. Uyama, Y. Otani, K. Fukamichi, O. Kitakami, Y. Shimada, J. Echigoya, *Appl. Phys. Lett.* 71 (1997) 1258.
- [4] M. Tsunoda, Y. Tsuchiya, M. Konoto, M. Takahashi, *J. Magn. Magn. Mater.* 171 (1997) 29.
- [5] H. Fuke, K. Saito, Y. Kamiguchi, H. Iwasaki, M. Sahashi, *J. Appl. Phys.* 81 (1997) 4004.
- [6] K. Hoshino, R. Nakatani, H. Hoshiya, Y. Sugita, S. Tsunashima, *Jpn. J. Appl. Phys.* 35 (1996) 607.
- [7] R.D. Lowde, R.T. Harley, G.A. Saunders, M. Sato, R. Scherm, C. Underhill, *Proc. Roy. Soc. A* 374 (1980) 87.
- [8] Y. Tsunoda, N. Oishi, N. Kunitomi, *Physica B* 119 (1983) 51.
- [9] Y. Endoh, Y. Ishikawa, *J. Phys. Soc. Jpn.* 30 (1971) 1614.
- [10] A. Kussmann, K. Müller, H. Wollenberger, *Z. Phys.* 20 (1966) 461.
- [11] E. Krén, G. Kádár, L. Pál, J. Sólyom, P. Szabó, *Phys. Lett.* 20 (1966) 331.
- [12] E. Krén, *Phys. Lett.* 21 (1966) 383.
- [13] E. Krén, G. Kádár, L. Pál, J. Sólyom, P. Szabó, T. Tarnóczy, *Phys. Rev.* 171 (1968) 574.
- [14] Y. Endoh, Y. Ishikawa, T. Shinjo, *Phys. Lett.* 29A (1969) 310.
- [15] Y. Ishikawa, Y. Endoh, *J. Appl. Phys.* 39 (1968) 1318.
- [16] T.J. Hicks, A.R. Pepper, J.H. Smith, *J. Phys. C* 1 (1968) 1683.
- [17] T.J. Hicks, J.D. Browne, *Proc. Phys. Soc.* 86 (1965) 139.
- [18] E. Raub, W. Mahler, *Z. Metallkde.* 46 (1995) 282.
- [19] J. Echigoya, private communication.
- [20] Y. Nakamura, M. Shiga, S. Kawano, *Physica B* 120 (1983) 212.
- [21] H. Yasui, T. Kaneko, H. Yoshida, S. Abe, K. Kamigaki, N. Mori, *J. Phys. Soc. Jpn.* 56 (1987) 4532.
- [22] T. Moriya, *Spin Fluctuations in Itinerant Electron Magnetism*, Springer-Verlag, Berlin, 1985.
- [23] K. Motizuki, H. Nagai, T. Tanimoto, *J. Phys. C* 8 (1988) 161.
- [24] S. Tomiyoshi, H. Yasui, T. Kaneko, Y. Yamaguchi, H. Ikeda, Y. Todate, K. Tajima, *J. Magn. Magn. Mater.* 90–91 (1990) 203.
- [25] T. Yamaoka, M. Mekata, H. Takaki, *J. Phys. Soc. Jpn.* 31 (1971) 301.
- [26] T. Yamada, N. Kunitomi, Y. Nakai, D.E. Cox, G. Shirane, *J. Phys. Soc. Jpn.* 28 (1970) 615.
- [27] T. Yamaoka, M. Mekata, H. Takaki, *J. Phys. Soc. Jpn.* 36 (1974) 438.
- [28] T. Yamaoka, *J. Phys. Soc. Jpn.* 36 (1974) 445.